The effect of iron on *Trichomonas vaginalis* TvCP2: a cysteine proteinase found in vaginal secretions of trichomoniasis patients

Luis Alberto Rivera-Rivas[1], Sebastián Lorenzo-Benito[1],
Diana Belén Sánchez-Rodríguez[1], Jesús FT Miranda-Ozuna[1],
Esly Alejandra Euceda-Padilla[1], Jaime Ortega-López[2], Bibiana Chávez-Munguía[1],
Anel Lagunes-Guillén[1], Beatriz Velázquez-Valassi[3], Lidia Jasso-Villazul[4]
and Rossana Arroyo[1] (iD)

[1]Departamento de Infectómica y Patogénesis Molecular, Centro de Investigación y de Estudios Avanzados del Instituto Politécnico Nacional (CINVESTAV-IPN), CP 07360, Mexico City, Mexico; [2]Departamento de Biotecnología y Bioingeniería, CINVESTAV-IPN, CP 07360, Mexico City, Mexico; [3]Departamento de Vigilancia Epidemiológica del Hospital General de México 'Eduardo Liceaga', CP 06720, Mexico City, Mexico and [4]Unidad de Medicina Preventiva del Hospital General de México 'Eduardo Liceaga', CP 06720, Mexico City, Mexico

Abstract

Trichomonas vaginalis (Tv) induces host cell damage through cysteine proteinases (CPs) modulated by iron. An immunoproteomic analysis showed that trichomoniasis patient sera recognize various CPs, also some of them are present in vaginal washes (VWs). Thus, the goal of this work was to determine whether TvCP2 is expressed during infection and to assess the effect of iron on TvCP2 expression, localization and contribution to *in vitro* cellular damage. Western-blotting (WB) assays using TvCP2r and vaginitis patient serum samples showed that 6/9 Tv (+) but none of the Tv (−) patient sera recognized TvCP2r. WB using an anti-TvCP2r antibody and VWs from the same patients showed that in all of the Tv (+) but none of the Tv (−) VWs, the anti-TvCP2r antibody detected a 27 kDa protein band that corresponded to the mature TvCP2, which was confirmed by mass spectrometry analysis. Iron decreased the amount of TvCP2 mRNA and the protein localized on the parasite surface and cytoplasmic vesicles concomitant with the cytotoxic effect of TvCP2 on HeLa cells. Parasites pretreated with the anti-TvCP2r antibody also showed reduced levels of cytotoxicity and apoptosis induction in HeLa cell monolayers. In conclusion, these results show that TvCP2 is expressed during trichomonal infection and plays an important role in the *in vitro* HeLa cell cytotoxic damage under iron-restricted conditions.

Introduction

Trichomonas vaginalis (Tv) is the protozoan parasite responsible for human trichomoniasis, the most common, non-viral, sexually transmitted neglected disease worldwide (WHO, 2012). This infection is associated with serious health complications, such as pregnancy outcome, children with low birth weight, infertility, and cervical and prostate cancer (Lehker and Alderete, 2000).

During infection, trichomonads are exposed to constantly changing microenvironmental conditions throughout the menstrual cycle, such as nutrients scarcity and competition with the vaginal microbiota, hit by the host immune response and hormonal fluctuations, among others. However, *T. vaginalis* has mechanisms that allow the parasite to adapt and respond to environmental changes, such as iron concentration differentially modulating the gene expression of virulence factors, among other proteins, thus allowing the maintenance of a chronic infection (Figueroa-Angulo *et al.*, 2012).

Trichomonas vaginalis has high requirements of exogenous iron (up to 300μM), an essential micronutrient for its survival, multiplication and metabolism (Gorrell, 1985; Lehker and Alderete, 1992). Iron by known and unknown mechanisms also regulates the virulence factors of *T. vaginalis*. The absence of iron in the culture media reduces cell growth and induces morphological changes in *T. vaginalis* from amoeboid to rounded parasites and flagella internalization. Evidence of pseudocyst formation in *T. vaginalis* under nutritional stress conditions such as iron restriction has been reported (Dias-Lopes *et al.*, 2017). Thus, iron plays an important role in the physiology and morphology of *T. vaginalis*. Besides, morphological alterations are also accompanied by an extensive change in the protein profiles of parasite grown under different iron conditions and suggest that protein synthesis is differentially regulated by iron in trichomonads (Benchimol, 2004; De Jesus *et al.*, 2006, 2007).

The *T. vaginalis* genome has ∼440 genes that encode proteinases; half of them are cysteine proteinases (CPs), and 48 correspond to cathepsin L-like CPs (Carlton *et al.*, 2007),

but less than half show proteolytic activity by two-dimensional gel electrophoresis (2-DE) zymography (Neale and Alderete, 1990; Ramón-Luing *et al.*, 2010; Cárdenas-Guerra *et al.*, 2013). The expression of some CP genes is differentially modulated by iron concentrations (Arroyo *et al.*, 2015). Moreover, CPs are considered to be virulence factors (Hernández *et al.*, 2014), participating in haemolysis (Dailey *et al.*, 1990; Fiori *et al.*, 1993, 1996, 1999; Lubick and Burgess, 2004; Cárdenas-Guerra *et al.*, 2013, 2015), complement resistance (Alderete *et al.*, 1995), cytoadherence (Arroyo and Alderete, 1989, 1995; Mendoza-López *et al.*, 2000; Rendón-Gandarilla *et al.*, 2013), cytotoxicity (Alvarez-Sánchez *et al.*, 2000, 2007; Ramón-Luing *et al.*, 2011; Carvajal-Gámez *et al.*, 2014; Arroyo *et al.*, 2015) and apoptosis induction in HeLa and human vaginal epithelial cells (Sommer *et al.*, 2005; Kummer *et al.*, 2008; Miranda-Ozuna *et al.*, 2019).

The *tvcp2* (TVAG_057000) gene (945-bp) was identified as one of the cDNA clones in an expression library together with three other genes that encode similar trichomonad cathepsin L-like CPs (Mallinson *et al.*, 1994), which were also found in *in vitro* secretion products (SPs) involved in the induction of apoptosis in vaginal epithelial cells (Sommer *et al.*, 2005). TvCP2 is downregulated by glucose and is involved in cellular damage (Miranda-Ozuna *et al.*, 2019). Moreover, several immunogenic proteinases from *T. vaginalis* (immunoproteome) were identified in an immunoproteomic analysis, combined with mass spectrometry (MS) and the use of patient sera in 2-DE-Western-blotting (2-DE-WB) assays (Ramón-Luing *et al.*, 2010). In this analysis, TvCP2 was one of the CPs recognized by patient sera. However, the presence of TvCP2 in vaginal secretions during infection and the effect of iron on the expression, localization and function of TvCP2 in the cytotoxic mechanisms of *T. vaginalis* and the putative association with cystatin-like endogenous CP inhibitors have not yet been determined.

In this work, we demonstrated the presence of TvCP2 in vaginal washes (VWs) of trichomoniasis patients and assessed the effect of iron in diminishing the expression of TvCP2, which is localized on the plasma membrane and in secretory vesicles, and could be targeted by TC-3, an endogenous CP inhibitor of *T. vaginalis*. TvCP2 is a key parasite CP involved in the cytotoxic cellular damage through apoptosis induction in HeLa cells under iron-restricted (IR) conditions.

Materials and methods

Cloning and expression of the TvCP2 recombinant protein

The complete *tvcp2* gene (945-bp) (TVAG_057000) was amplified by PCR using trichomonad genomic DNA as a template, a sense primer (5′-GCCGGTACCATGTTTGCTTTCTTGCTTTCTGGC-GCT-3′), and an antisense primer (5′-GGCGAATTCTTAGAG-AGCCTTTGGAAGGATAGTTCAG-3′) (Supplementary Fig. S1A). The restriction sites used, *Kpn*I and *Eco*RI, respectively, are underlined in the primer sequences for directional cloning into the pCold I prokaryotic expression vector (Takara Bio Inc., Mountain View, CA, USA), as recommended by the manufacturer. Recombinant protein expression in the *Escherichia coli* strain BL21 (DE3) was induced with 1 mM isopropyl-β-D-1-thiogalatopyranoside for 16 h at 16 °C and analysed by sodium dodecyl sulphate polyacrylamide gel electrophoresis (SDS-PAGE) and WB assays using an anti-histidine6 tag monoclonal antibody (α-His6; Invitrogen-Gibco, Carlsbad, CA, USA). The recombinant TvCP2 protein (TvCP2r) was purified by affinity chromatography using Ni-Sepharose 6 Fast Flow columns (GE Healthcare-Amersham Biosciences, UK), as recommended by the manufacturer (Supplementary Fig. S2A).

Production of a polyclonal anti-TvCP2r antibody (anti-TvCP2r)

To produce an anti-TvCP2r polyclonal antibody, a 6-week-old male New Zealand rabbit was subcutaneously immunized twice with 200 μg of purified TvCP2r protein mixed with the TiterMax Gold adjuvant (Sigma-Aldrich, Co., St. Louis, MO, USA) every 15 days. The anti-TvCP2r antibody was used in WB assays to detect native TvCP2 in VWs from patients with trichomoniasis and in Tv extracts, for indirect immunofluorescence, and for cytotoxicity and apoptosis-induction inhibition assays. A preimmune (PI) serum sample was obtained before animal immunization and was used as a negative control in all experiments using antibodies (Supplementary Fig. S2B and C). For inhibition assays, immunoglobulin G (IgG) fractions from anti-TvCP2r and PI sera were obtained using the caprylic acid method (Harlow and Lane, 1988). The use and handling of rabbits for antibody production were included in a protocol submitted and approved by the Institutional Animal Care and Use Committee at CINVESTAV (Protocol No. 0229-16).

Biological samples

To detect the presence of TvCP2 in VWs from patients with trichomoniasis, nine Tv (+) VWs and nine Tv (−) samples were obtained from patients attending the Hospital General de México (HGM), who had been diagnosed with vaginitis through clinical examination. Diagnosis for the presence or absence of Tv in these patients was confirmed by VW microscopic analysis and *in vitro* culture (Table 1). Moreover, to detect the presence of antibodies against TvCP2 in sera from patients with trichomoniasis, TvCP2r was used as an antigen in WB assays, and sera from Tv (+) and Tv (−) patients were used as primary antibodies (1:100 dilution) (Table 1). To obtain patient biological samples (VW and serum), each patient who participated in this study signed an informed consent form included in a protocol approved by the HGM scientific and ethical committees (Protocol No. DI/14/204/03/010).

Parasites and HeLa cell cultures

Parasites from the fresh clinical *T. vaginalis* isolates CNCD 147 (type 2) and CNCD 280 (type 1) were used in this study for all experiments or where indicated, respectively (Alvarez-Sánchez *et al.*, 2000; Conrad *et al.*, 2012; Sánchez-Rodríguez *et al.*, 2018). Trichomonad cultures were maintained at 37°C for 1 week by daily passage in trypticase-yeast-extract-maltose (TYM) medium supplemented with 10% heat-inactivated bovine serum (HIBS) (Diamond, 1957). Organisms at the mid-logarithmic phase were used for all assays. The TYM medium used for regular parasite growth contained 20 μM iron [normal iron (NI) condition]. For parasites grown under high-iron (HI) or IR condition (250 or 0 μM iron, respectively), the culture medium was supplemented with 250 μM ferrous ammonium sulphate or 150 μM 2-2′-dipyridyl (an iron-chelating agent; Sigma-Aldrich, Co.), respectively (Gorrell, 1985; Alvarez-Sánchez *et al.*, 2007). To obtain confluent HeLa cell monolayers, cells were grown in Dulbecco's modified Eagle medium (DMEM) (Gibco Lab, Grand Island, NY, USA) supplemented with 10% HIBS at 37 °C for 48 h in a 5% CO_2 atmosphere (Alvarez-Sánchez *et al.*, 2000; Miranda-Ozuna *et al.*, 2019).

RNA isolation and reverse transcription polymerase chain reaction (RT-PCR) analysis

Total RNA was isolated from parasites (2×10^7) grown under different iron concentrations using TRIzol reagent (Invitrogen). The quality of RNA was determined using agarose gels (data not shown). Before cDNA synthesis, total RNA was first treated with

Table 1. Characteristics of biological samples from patients with vaginitis used in Western-blot assays shown in Fig. 1

| Sample number[a] | Patient ID | VW microscopic analysis[b] | | | | Tv culture | Serum[c] |
		VEC[d]	WBC[e]	Bacteria	Tv[f]		
1	HGMM 718	+	+	+++	+	+	+
2	HGMM 513	+	++	+++	+	+	+
3	HGMM 664	++	+	+++	+	+	+
4	HGMM 492	+	+	+	+	+	+
5	HGMM 507	+	+	++	+	+	+
6	HGMM 588	+	+++	+	+	+	+
7	HGMM 490	+	++	++	+	+	+
8	HGMM 478	++	+	+++	+	+	+
9	HGMM 615	+	+	+	+	+	+
10	HGMM 578	+	+	+++	–	–	+
11	HGMM 479	+	++	+++	–	–	+
12	HGMM 261	++	+	+++	–	–	+
13	HGMM 431	+	+	+	–	NA	–
14	HGMM 367	+	+	++	–	NA	–
15	HGMM 457	+	+++	+	–	NA	–
16	HGMM 452	+	++	++	–	NA	–
17	HGMM 717	++	+	+++	–	NA	–
18	HGMM 587	+	+	+	–	NA	–

Samples of vaginal washes (VWs) and sera were obtained from enrolled people attending for an annual Pap smear examination at the 'Medicina Preventiva del Hospital General de México' (HGMM). People accepted to participate after signing the consent form approved in the Protocol No. DI/14/204/03/010 by the HGM ethical committee. The presence of Tv detected in the microscopic analysis was confirmed by *in vitro* culture of vaginal secretions. All patients were diagnosed with cervicovaginitis, but in none of them was the presence of yeast detected.
[a]The patient sample number from 1 to 9 of WVs and sera are from Tv (+) patients and from 10 to 18 are from Tv (−) patients. These samples were used in WBs shown in Fig. 1.
[b]Patient WVs were TCA-precipitated for the WB assay presented in Fig. 1C using anti-TvCP2r serum as the primary antibody. The protein profile of each VW used in Fig. 1C was shown as Supplementary Fig. S4. Signs (+ or −) show the abundance of cellular components as follows: +, few; ++, moderate; +++ abundant; −, absent.
[c]Patient serum at 1:100 dilution for the WB assay presented in Fig. 1B using TvCP2r as antigen; NA, no serum sample was obtained from these patients.
[d]VEC, presence of vaginal epithelial cells.
[e]WBC, presence of white blood cells.
[f]Tv, presence of moving parasites confirmed by *in vitro* culture of VW.

DNase I for 60 min at 37°C. To check for the absence of gDNA, DNase-treated RNA was used as a template for PCR reaction. PCR reaction without cDNA was also used as a negative control (Fig. 2A). To obtain cDNA, 10 μg total DNase-treated RNA was processed using a RevertAid first-strand cDNA synthesis kit (Thermo Scientific-Pierce, Rockford, IL, USA), following the manufacturer's instructions. For endpoint PCR amplification, 500 ng cDNA, *Taq* DNA polymerase (Invitrogen) and specific primers for *tvcp2* (TVAG_057000) designed using the gene sequence reported in TrichDB were selected to amplify a 322-bp fragment. The *tvcp2* primers used were a sense primer (5′-GGGCTACG-ATGAGGTTAAGG-3′) at position 623–643 nt and an antisense primer (5′-GGCGAATTCTTAGAGAGCCTTTGGAAGGATAG-TTCAG-3′) at position 908–945 nt (Supplementary Fig. S1A). The amplification programme consisted of 20 cycles of denaturation at 95 °C for 1 min, annealing at 55 °C for 35 s and extension at 72 °C for 80 s. The 112-bp fragment of the *T. vaginalis β-tubulin* mRNA (Madico *et al.*, 1998) was used as an internal control. The amplification programme consisted of 25 cycles of denaturation at 94 °C for 1 min, annealing at 55 °C for 1 min and extension at 72 °C for 30 s. These experiments were performed three independent times with similar results.

Protein preparation and SDS-PAGE

Proteins [total protein extracts (TPEs) and protease-resistant extracts (PREs)] were obtained from 2×10^7 parasites cultured under different iron concentrations. To obtain TPEs for WB, washed parasites were resuspended in PBS pH 7.0 for 10% trichloroacetic acid (TCA) precipitation at 4°C for 18 h. To obtain PREs for WB, washed parasites were lysed with 0.5% sodium deoxycholate in PBS pH 8.0, and in the absence of protease inhibitors to keep the proteolytic activity intact, as previously described (Miranda-Ozuna *et al.*, 2019). Then, PRE lysates were centrifuged at 13 000 × g for 30 min at 4°C and supernatants were analysed, without boiling, by SDS-PAGE on 12% polyacrylamide gels. Proteins from VWs were obtained by 10% TCA precipitation using 100 μL of VW supernatant. TCA-protein pellets from TPEs and VWs were resuspended directly in SDS-PAGE sample buffer, boiled for 3 min and analysed through SDS-PAGE and WB assays using different primary antibodies.

In vitro secretion assays

The *in vitro* secretion assay was performed as previously described (Hernández-Gutiérrez *et al.*, 2004) with some modifications. Briefly, parasites grown under IR or HI conditions were harvested, washed three times with PBS, resuspended (2×10^6 parasites mL^{-1}) in PBS-0.5% maltose directly or supplemented with 250 μM ferrous ammonium sulphate, according to the parasite growth condition (IR or HI, respectively), incubated for 90 min at 37 °C, and parasite viability was assessed by the Trypan Blue exclusion method. To confirm the presence of TvCP2 in the SPs, the supernatant was clarified by centrifugation at 900 × g,
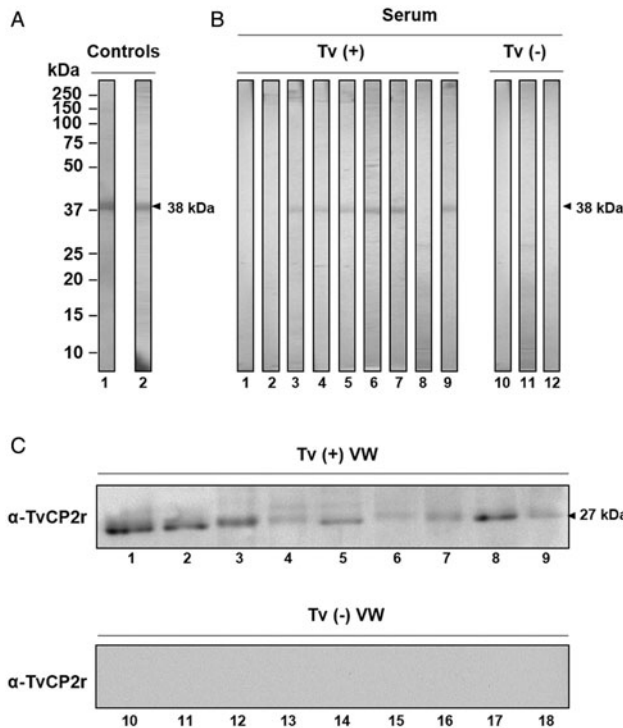
Fig. 1. Presence of TvCP2 during trichomonal infection. (A) Controls of WB assays using the recombinant TvCP2 protein (TvCP2r) transferred onto NC membrane stained with Ponceau Red (lane 1) and the recognition by the anti-TvCP2r antibody (1:8000 dilution; lane 2) used as a positive control. (B) WB assays using NC membrane containing TvCP2r as antigen incubated with different Tv (+) (lanes 1–9) and Tv (−) (lanes 10–12) patient sera (Table 1) at a 1:100 dilution. (C) WB assays performed using the anti-TvCP2r (1:2000 dilution) antibody in NC membranes containing duplicate samples of the proteins from nine Tv (+) (Supplementary Fig. S3, lanes 1–9) and nine Tv (−) vaginal washes (VWs) (Supplementary Fig. S3, lanes 10–18) previously separated by SDS-PAGE using 12% polyacrylamide gels and CBB-stained (Supplementary Fig. S3; Table 1). Sera and VWs used in Fig. 1B and C, lanes 1–12 are from the same patients in each case (Table 1).

filtered through a 0.22 μm membrane, and proteins were precipitated with 10% TCA at 4°C for 18 h prior to WB assays. These experiments were performed at least in three independent times.

Western blot

WB assays were performed using different sources of proteins (TvCP2r, *in vitro* SPs, TPEs or PREs from Tv or TCA-precipitated proteins from VWs) separated by SDS-PAGE on 12% polyacrylamide gels, transferred onto nitrocellulose (NC) membranes (0.2 μm pore size; Bio-Rad Laboratories, Hercules, CA, USA), and blocked with 10% non-fat dried milk in PBS-0.1% Tween 20 (PBS-T20). The NC membranes were incubated for 1 h at 37°C with the following primary antibodies diluted in PBS-T20: anti-TvCP2r (1:2000 dilution); anti-TvCP4r (1:500 dilution; Cárdenas-Guerra et al., 2013), TvCP4 is a CP that is secreted under HI conditions and was used as a positive control for SPs; anti-TvPFOr (1: 10 000 dilution; Meza-Cervantez et al., 2011), this antibody was produced against a recombinant protein of the carboxy-terminal region of Tv pyruvate ferredoxin:oxidoreductase (PFO) A, which is induced under HI condition and was used as a positive control for iron induction; anti-EhHKr (1:500 dilution; Meza-Cervantez et al., 2011), this antibody was produced against an *Entamoeba histolytica* hexokinase recombinant protein (EhHKr) that recognizes the TvHK, which was used as a negative control for SPs WB; anti-TvLEGU-1r (1:500 dilution; Rendón-Gandarilla et al., 2013), TvLEGU-1 is a CP of the asparaginyl endopeptidase (legumain) subfamily that was used as a

loading control for PREs WB; anti-His6 (1:1000 dilution), PI serum (1:100 dilution) or Tv (+) and Tv (−) patient sera (dilution 1:100; Ramón-Luing et al., 2010). After five washes with PBS-T20, NC membranes were incubated for 1 h at 37°C with a peroxidase-conjugated goat anti-rabbit, anti-mouse or anti-human IgG secondary antibody (1:3000 dilution; Bio-Rad Laboratories). Then, the reactive bands were developed using a chemiluminescence system (SuperSignal West Pico Chemiluminescent Substrate, Thermo Scientific-Pierce), images were captured in a ChemiDoc XRS System (Bio-Rad), and analysed using Quantity One software (Bio-Rad). Densitometry analysis was determined using the pixels of the TvCP2 protein bands detected by the anti-TvCP2r antibody in the IR conditions as a 100% intensity and used to calculate the relative intensity of the bands detected by the anti-TvCP2r antibody in the HI conditions for both types of protein extracts (TPEs and PREs) and the *in vitro* secretion assay. These experiments were performed at least in three independent times.

Protein identification by MS

Protein bands of interest detected in WB assays using *in vitro* trichomonad SPs and patient VWs were excised from Coomassie brilliant blue (CBB)-stained gels (Supplementary Fig. S4). The samples were analysed on a NanoAcquity nano-flow liquid chromatography (LC) system (Waters), coupled to a linear ion trap mass spectrometer (Thermo Fisher Scientific, Bremen, Germany) equipped with a nanoelectrospray ion source (LC-ESI-MS/MS). Proteins were identified from the tandem MS data using SEQUEST software with searches in the TrichDB database at the Proteomics Laboratory in CINVESTAV-Unidad Irapuato.

Indirect immunofluorescence assay (IFA) and lysotroger labelling assays

To determine the cellular localization of TvCP2 under different iron concentrations, IFA and confocal microscopy analyses were performed using parasites grown under IR and HI conditions and an anti-TvCP2r antibody. Parasites attached to coverslips were fixed with 4% formaldehyde in PBS for 30 min at room temperature (RT). Half of the coverslips with fixed parasites were permeabilized with 0.07% Triton X-100 for 5 min at RT, while the other half were not treated. All coverslips were then blocked with 0.5 M glycine for 1 h at 37 °C and 1% fetal bovine serum for 15 min at 37 °C. Parasites were incubated with the anti-TvCP2r antibody or PI serum as a negative control (1:100 dilution) for 18 h at 4 °C, followed by incubation with a fluorescein isothiocyanate (FITC)-conjugated secondary anti-rabbit antibody (1:100 dilution) (Thermo Scientific-Pierce) for 1 h at RT. The parasites were stained with the membrane marker 1,1′-Dioctadecyl-3,3,3′,3′-tetramethylindocarbocyanine perchlorate (DIL-CM-38; Molecular Probes-Invitrogen) at 1:2000 dilution for 30 min at RT, washed with PBS, and mounted with Vectashield-DAPI (4′,6-Diamidine-2′-phenylindole dihydrochloride; Vector Laboratories, Burlingame, CA, USA) mounting solution. For lysosomal co-localization assays, the acidic compartments of live parasites grown under both iron conditions (IR and HI) were incubated with 2 μM LysoTracker Red DND-99 (Invitrogen) following the manufacturer's instructions for 30 min at 37 °C. Parasites were then washed, fixed and processed as previously described by Miranda-Ozuna et al. (2019) for IFA and incubated with an anti-TvCP2r antibody.

The TC-3 and TvCP2 co-localization assays were performed using the CNCD280 Tv isolate, as previously reported (Sánchez-Rodríguez et al., 2018). Briefly, parasites were incubated with both primary antibodies (mouse anti-TC-3r and rabbit anti-TvCP2r, both at 1:100 dilution) for 18 h at 4 °C, washed
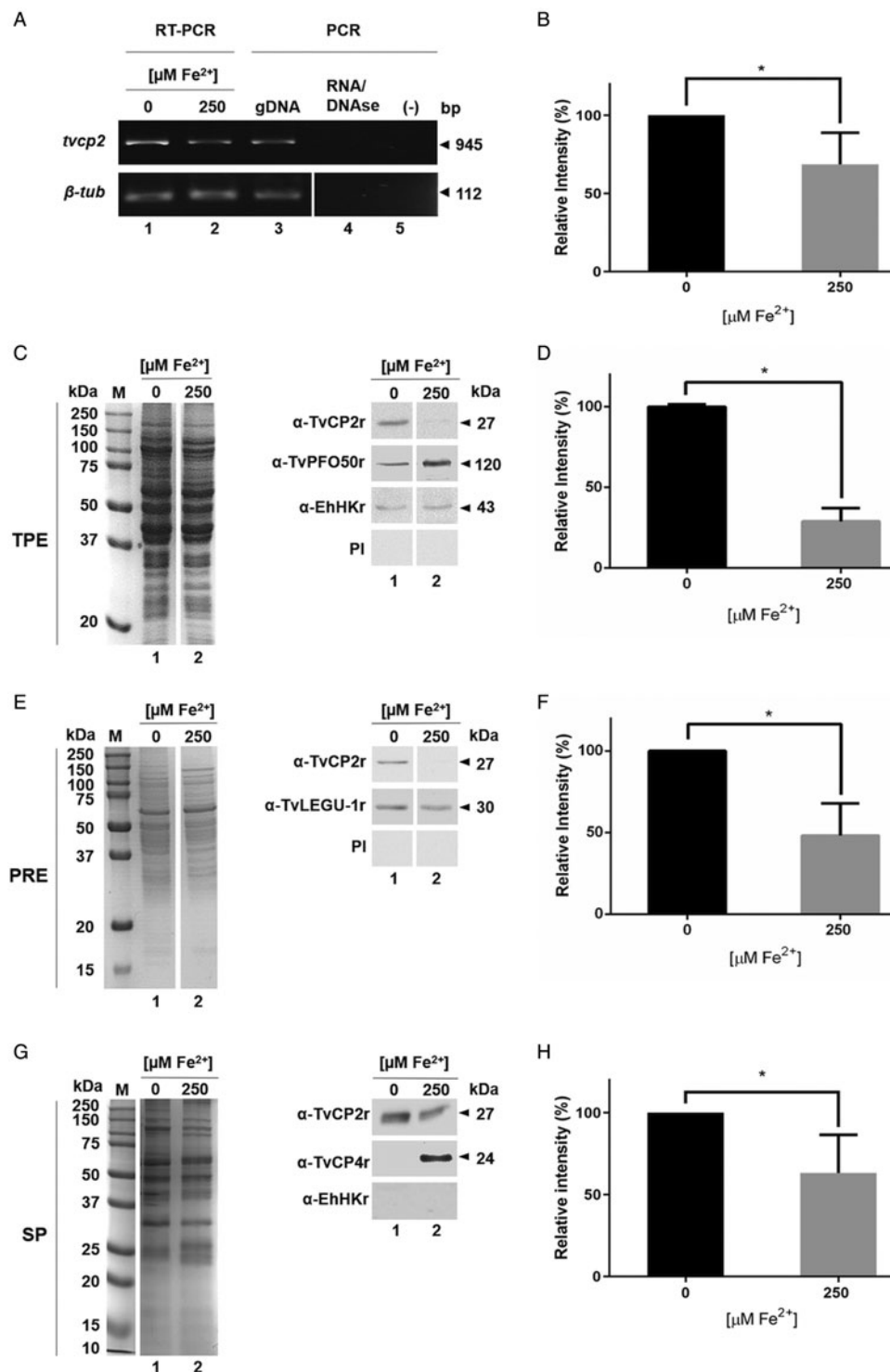
Fig. 2. Effect of iron on the expression of TvCP2 at the mRNA, protein and *in vitro* secretion. (A) Endpoint RT-PCR with specific primers for the *tvcp2* and *β-tubulin* genes using 500 ng of cDNA from parasites grown in IR (0 μM; lane 1) and HI conditions (250 μM; lane 2). As a positive control, 500 ng of gDNA was used (lane 3). To verify the lack of gDNA contamination, DNase-I-treated RNA was used as a template for the PCR (lane 4). As another negative control, a reaction without DNA was used (lane 5). *β-*Tubulin mRNA under different iron concentrations was used as a loading control. Arrowheads show the length of each amplicon in base pairs (bp). (B) Densitometric analysis of the *tvcp2* bands detected in the ethidium bromide-stained agarose gel in (A) using Quantity One software (Bio-Rad) and compared with the *β-tubulin* bands used as a loading control. (C and E) Coomassie-Brilliant-Blue (CBB)-stained 12% SDS-PAGE gel for TPEs and PREs from parasites grown under IR (0 μM) and HI (250 μM) conditions (lanes 1 and 2), respectively. For WB assays, duplicate gels of (C) and (E) were transferred onto NC membranes and incubated with different antibodies: anti-TvCP2r polyclonal antibody (1:2000 dilution); anti-TvPFO50r antibody (1: 10 000 dilution) to detect an overexpressed PFO-A control protein under HI conditions; anti-EhHKr antibody (1:1000 dilution) as a loading control to detect TvHK; anti-TvLEGU-1r antibody (1:500 dilution) as a control for a proteinase expressed under both iron conditions used; and PI serum (1:1000 dilution) as a negative control. (D and F) Densitometric analysis of the TvCP2 protein bands detected by WB in (C and E) using Quantity One software (Bio-Rad) were compared with the protein bands detected by the anti-EhHKr antibody in (C) and by the anti-TvLEGU-1r antibody in (F) as loading controls, respectively. (G) CBB-stained protein profiles of the *in vitro* secreted products from parasites grown under IR (0 μM) and HI (250 μM) conditions. WB assay of duplicated samples transferred onto NC membranes using polyclonal antibodies specific for each protein (anti-TvCP2r, anti-TvCP4r and anti-EhHKr) to detect TvCP2; TvCP4 (secreted protein) and TvHK (non-secreted protein) were used as controls to determine the active secretion of TvCP2 from live parasites. (H) Densitometric analysis of the protein bands detected by WB in (G) for TvCP2 using Quantity One software (Bio-Rad). The band detected by amplification of *tvcp2* by RT-PCR and TvCP2 in WB assays with the anti-TvCP2r antibody in the IR-grown parasite TPE, PRE or SP (A, C, E and G) was set as 100% of relative intensity for the densitometry analysis (B, D, F and H). (*) indicate a significant difference with $P < 0.05$ values.

with PBS, incubated with FITC-conjugated and Alexa-Fluor-594-conjugated secondary antibodies, respectively (1:100 dilution; Thermo Scientific-Pierce) for 1 h at RT, mounted, and analysed by confocal microscopy using a Zeiss microscope and Zen 2012 software (Carl Zeiss, Germany). PI sera were used as negative controls. To quantify the degree of co-localization (putative molecular association) between two fluorochromes, the Pearson's correlation coefficient (r) was used. Values close to zero represent weak association while values between 0.5 and 1 represent biological meaningful association (Adler and Parmryd, 2010).

Pull-down assay

A pull-down assay was performed according to the manufacturer's instructions (Pierce™ Pull-Down PolyHis Protein: Protein Interaction Kit) as recently reported (Sánchez-Rodríguez et al., 2018). Briefly, TC-3r and clarified protein extract (CPE) were used as bait and prey proteins, respectively. The CPE was obtained from parasites (2×10^7) of the CNCD 280 isolate grown under NI conditions. The CPE was incubated with TC-3r (150 μg) previously immobilized on a cobalt resin column for 18 h at 4°C. After washing, fractions (CPE, washes and bound or prey proteins) were analysed by SDS-PAGE on a 13% polyacrylamide CBB-stained gel. Additionally, bound proteins were transferred onto NC membranes (Bio-Rad) for WB detection with the anti-TvCP2r antibody and with the anti-TvTIMr antibody and PI serum as negative controls (Sánchez-Rodríguez et al., 2018). Bovine serum albumin (BSA) and HSP70r were used as a negative control and unrelated protein, respectively, with a similar treatment as TC-3r.

Immunogold localization using transmission electron microscopy (TEM)

These assays were performed using the CNCD280 Tv isolate, as previously reported (Sánchez-Rodríguez et al., 2018), grown under NI conditions. Ultrathin (60 nm) sections were obtained and incubated for 18 h at RT with a mouse anti-TC-3r antibody (1:10 dilution) or with a rabbit anti-TvCP2r antibody (1:20 dilution) alone or together (for co-localization assays) with mouse anti-TC-3r as primary antibodies, and with gold-conjugated anti-mouse or anti-rabbit IgG (1:60 dilution) (or together) as secondary antibodies (Ted Pella Inc. Redding, CA, USA) (using 20 or 30 and 15 nm gold particles, respectively). Then, the sections were contrasted with uranyl acetate and lead citrate. Secondary antibodies alone were used as negative controls for these assays. The sections were examined using a JEM-1011 transmission electron microscope (JEOL Ltd., Tokyo, Japan).

Cytotoxicity, apoptosis induction and inhibition assays

Cytotoxicity assays were performed by a colorimetric method as previously described (Alvarez-Sánchez et al., 2000; Miranda-Ozuna et al., 2019) using confluent HeLa cell monolayers in 96-well microtiter plates and parasites grown under IR or HI conditions. For inhibition assays, parasites grown under IR conditions were incubated prior to the interaction assays for 30 min at 4 °C in the presence of increasing IgG concentrations (0, 50, 100 and 300 μg mL^{-1}) of anti-TvCP2r or PI serum (used as a negative control). The parasites were then washed and resuspended in interaction medium (DMEM: iron-chelated TYM at a 2:1 ratio and without serum). The untreated or IgG-pre-treated parasites (2×10^5 well^{-1}) were added to confluent HeLa cell monolayers (5×10^4 well^{-1}) at a 5:1 parasite-to-host cell ratio and incubated for 1 h at 37°C in a 5% CO_2 atmosphere. HeLa cell monolayer destruction was assessed using light microscopy and spectrophotometric

quantification at 570 nm. Untreated parasites were set as 100% cytotoxicity. Each experiment was performed in triplicate at least three independent times, with similar results.

Trichomonal apoptosis induction assays: Terminal Deoxynucleotidyl Transferase-mediated dUTP Nick-End Labeling (TUNEL) DNA fragmentation and Annexin V-FITC were performed. A TUNEL assay after the cytotoxicity assay in the absence or presence of 300 μg mL^{-1} anti-TvCP2r IgG-treated parasites using the DeadEnd™ Fluorometric TUNEL System (Promega, Madison, WI, USA) was performed following the manufacturer's instructions. Briefly, after incubation of T. vaginalis with confluent HeLa cell monolayer for 30 min at 37 °C, cells recovered from the supernatant and those remaining in the monolayer attached to the coverslips were fixed with 4% formaldehyde, permeabilized with 0.2% Triton X-100 for 5 min at RT, and incubated with the Terminal deoxynucleotidyl transferase and fluorescein-labelled nucleotide mix for 1 h at 37°C. Nuclei were stained with DAPI. HeLa cells and Tv incubated with H_2O_2 for 30 and 60 min at 37 °C in a 5% CO_2 atmosphere were used as positive controls. Green fluorescence incorporated in the nicked DNA was observed by confocal microscopy (Zeiss). Experiments were performed at least two independent times with similar results.

To confirm the role played by TvCP2 in apoptosis induction, other assays were also performed. For the DNA fragmentation assay, after incubation of T. vaginalis (with or without pre-treatment with anti-TvCP2r or PI IgGs) with confluent HeLa cell monolayers on six-well microtiter plates for 30 min at 37 °C in a 5% CO_2 atmosphere, the supernatant was recovered and centrifuged. The cells attached to the plate and in the pellet were processed for DNA extraction as previously reported (Miranda-Ozuna et al., 2019). As positive controls, parasites and HeLa cells treated with 5% H_2O_2 for 30 and 60 min at 37 °C in a 5% CO_2 atmosphere were used. The DNA was analysed by electrophoresis in 2% agarose gels. The experiments were performed at least two independent times with similar results.

For the annexin V-FITC staining method, after the incubation of T. vaginalis with confluent HeLa cell monolayers for 30 min at 37 °C in a 5% CO_2 atmosphere, the cell monolayers were labelled with the Annexin V-FITC Fluorescence Microscopy Kit (BD Pharmingen) for 15 min at RT, following the manufacturer's recommendations. The FITC fluorescent signal from apoptotic HeLa cells was observed under an epifluorescence inverted microscope (Nikon, Japan) and quantified by a spectrofluorometric analysis (SpectraMax Gemini EM spectrofluorometer). The interaction of HeLa cell monolayers with parasites grown under IR conditions without antibody pre-treatment and their level of Annexin V label was set as 100% apoptosis.

Statistical analysis

Statistically significant differences between means were determined by analysis of variance (ANOVA) using GraphPad Prism 6. The scores showing statistical significance are indicated in the figures with asterisks. The corresponding P values are indicated in the figure legends.

Results

Expression of TvCP2r and anti-TvCP2r antibody production and validation

To demonstrate the expression of TvCP2 during trichomonal infection, we determined the immunogenicity of TvCP2 by detecting the reactivity of anti-TvCP2 antibodies in patient serum samples and the presence of the TvCP2 proteinase in vaginal secretions of patients with trichomoniasis using VWs

(Table 1). For this purpose, the recombinant TvCP2 protein and the previously generated polyclonal anti-TvCP2r antibodies (Miranda-Ozuna *et al.*, 2019) were used. The complete 945-bp open reading frame of the *tvcp2* gene (TVAG_057000) that encodes a 315-aa cathepsin L-like zymogen with a predicted molecular mass of ∼35 kDa and *pI* 7.0 (Supplementary Fig. S1A) was cloned. The N-terminal region from aa residues 1–72 corresponds to the prepro-region that is removed by proteolytic processing during proteinase maturation leaving a 242-aa and 27 kDa mature proteinase (Supplementary Fig. S1B). The affinity-purified recombinant TvCP2 (TvCP2r) proteinase expressed as a 38 kDa protein band (Supplementary Fig. S2A) was used as an antigen in WB assays with vaginitis patient sera (Fig. 1).

The anti-TvCP2r antibody produced in rabbits was validated by WB assays using TvCP2r, TPEs and PREs obtained from normally grown parasites (Supplementary Fig. S2). The anti-TvCP2r antibody recognized a 38 kDa TvCP2r protein band (Supplementary Fig. S2C, lane 1) and a ∼27 kDa protein band in the TCA-precipitated TPEs and the PREs from parasites grown in NI concentrations (Supplementary Fig. S2C, lanes 2 and 3). The ∼27 kDa protein could correspond to the mature TvCP2 proteinase (Supplementary Fig. S1B). The PI serum showed no reactivity (Supplementary Fig. S2B). The anti-TvCP2r antibody tested by IFA using normally grown fixed and non-permeabilized parasites detected TvCP2 mainly in spots on some parts of the parasite surface (Supplementary Fig. S2D).

TvCP2 is present during trichomonal infection

To determine the immunogenicity of TvCP2 during infection, the presence of anti-TvCP2 antibodies in vaginitis patient sera (Table 1) using TvCP2r as an antigen was analysed in WB assays. Figure 1B shows the immunodetection of TvCP2r (38 kDa) in 6/9 tested Tv (+) patient sera, while no bands were detected when Tv (−) patient sera were tested. As a positive control, the rabbit anti-TvCP2r antibody was used (Fig. 1A).

The presence of TvCP2 during infection in Tv (+) and Tv (−) VWs with similar cytological composition, at least under the microscopic examination of each wet mount (Table 1) was also analysed in WB assays. Proteins from VWs of vaginitis patients were concentrated by TCA precipitation, electrophoresed (Supplementary Fig. S3), and transferred onto NC membranes to perform WB assays using the anti-TvCP2r antibody (Fig. 1C). Supplementary Figure S3 shows the CBB-stained protein profile of each VW sample used in the WB analysis. The immune detection of TvCP2 in the Tv (+) VWs showed a 27 kDa protein band in all VWs tested (Fig. 1C), which was confirmed by MS analysis, using two bands from the 27 kDa region of Tv (+) and two from the Tv (−) VWs profiles (Supplementary Fig. S3, segmented rectangles). Only on the Tv (+) VWs bands, four peptides were identified that corresponded to the TVAG_057000 gene product, giving a 17% sequence coverage (Supplementary Fig. S1C). As expected, the anti-TvCP2r antibody did not detect the presence of TvCP2 in Tv (−) VWs (Fig. 1C). Thus, these data demonstrate that TvCP2 is expressed during infection.

TvCP2 is downregulated by iron at the mRNA and protein levels

The presence of TvCP2 in VWs of Tv (+) patients prompted us to study the effect of iron on the *in vitro* TvCP2 expression. Thus, the iron effect at the transcript and protein levels and in the *in vitro* secretion and cellular localization of TvCP2 was determined. The role of TvCP2 in parasite cytotoxicity was also analysed. These results could help explain its presence and function during infection when exposed to iron variations throughout the menstrual cycle.

To determine the effect of iron on the expression of *tvcp2*, we designed specific primers (Supplementary Fig. S1A) and performed an RT-PCR assay of the *tvcp2* gene using cDNA synthesized from DNase I-treated total RNA obtained from parasites grown under IR and HI conditions using trizol. RT-PCR results showed more *tvcp2* transcripts in the IR condition than in the HI condition (Fig. 2A), which was confirmed by a densitometry analysis (Fig. 2B). As a positive control, the *tvcp2* gene was amplified from genomic DNA, and *β*-tubulin mRNA was used as a loading control. DNase I-treated RNA as a template (no RT reaction) and a PCR reaction without DNA template were used as negative controls, which did not show any amplification (Fig. 2A, lanes 4 and 5).

To determine the effect of iron on TvCP2 protein expression, WB assays using TPEs from parasites grown in IR and HI conditions were performed. The anti-TvCP2r antibody recognized a 27 kDa protein band with greater intensity in parasites grown in IR conditions than in those grown under HI conditions (Fig. 2C and D). The anti-TvPFO50r antibody detected a 120 kDa PFO protein (used as a control for an iron-upregulated protein, PFO) (Meza-Cervantez *et al.*, 2011) with greater intensity in the HI condition than in the IR condition. The anti-EhHKr antibody [obtained against a recombinant hexokinase (EhHKr) from *E. histolytica* that recognizes Tv hexokinase (TvHK), which is a cytoplasmic protein that is not secreted *in vitro* and does not change under different iron conditions] detected a 43 kDa TvHK protein band with similar intensity in both iron conditions, which was used as a loading control. The PI serum used as a negative control showed no recognition, as expected (Fig. 2C and D). Also, WB assays using protein extracts prepared in the absence of protease inhibitors (PREs) from trichomonads grown under different iron conditions (Fig. 2E and F) were performed. The anti-TvCP2r antibody also detected a 27 kDa protein band with greater intensity in the IR condition than in the HI condition, compared with the recognition observed by the anti-TvLEGU-1r antibody (TvLEGU-1 is an asparaginyl endopeptidase that does not change under different iron conditions), a protein that was used as a loading control for PREs. The PI serum did not show any reactivity (Fig. 2E and F).

To corroborate that TvCP2 was present in Tv (+) vaginal secretions due to active secretion by live parasites under different iron concentrations, *in vitro* secretion assays under IR and HI conditions, WB assays using the anti-TvCP2r antibody and MS analysis to confirm the presence of TvCP2 were also performed. Parasite viability assessed during the *in vitro* secretion assay was 98 and 99% under IR and HI conditions, respectively. Figure 2G shows the presence of TvCP2 in the excretion products/SPs of live parasites, mainly under IR conditions, as supported by a densitometric analysis (Fig. 2H). Four peptides of the TVAG_057000 gene product were identified by MS, giving a 17% sequence coverage (Supplementary Fig. S1C). These data confirm the secretion of TvCP2 by metabolically active parasites mainly under IR conditions.

Localization of TvCP2

To determine whether iron modulates the subcellular localization of TvCP2, an IFA using the anti-TvCP2r antibody and fixed and non-permeabilized or permeabilized parasites grown under different iron conditions were performed and analysed by confocal microscopy. Figure 3 shows a higher TvCP2 fluorescence signal (in green) in IR than in HI parasites (Fig. 3A and B, panels d and i). TvCP2 was detected in spots on the surface of non-permeabilized parasite that co-localized (in yellow)
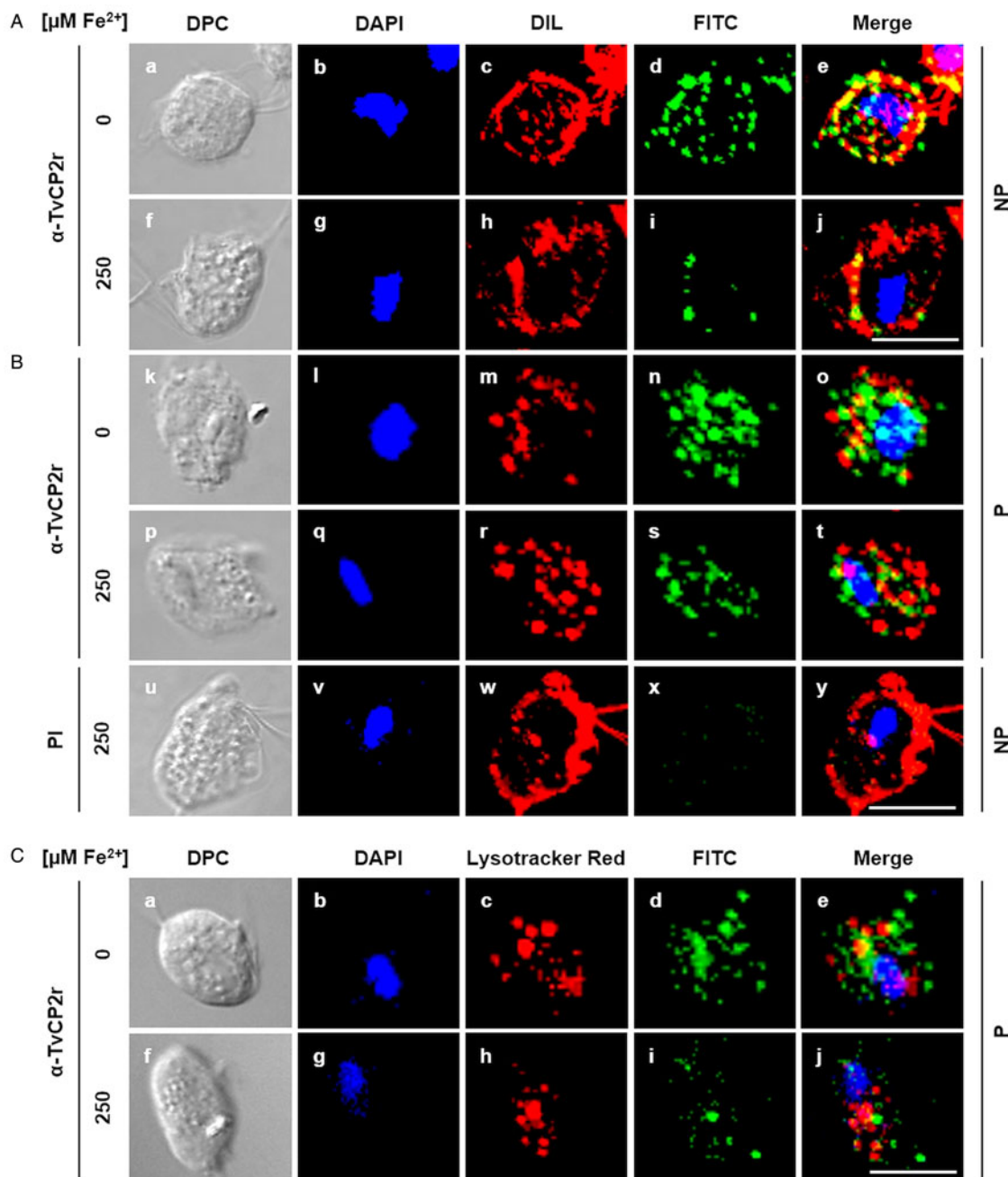
Fig. 3. TvCP2 is localized in spots on the parasite surface and in cytoplasmic vacuoles of *T. vaginalis* under different iron concentrations. (A and B) IFA of non-permeabilized (NP) and permeabilized (P) parasites, respectively, incubated with the anti-TvCP2r antibody followed by FITC-conjugated goat anti-rabbit IgG (in green). Differential phase contrast (DPC; a, f, k and p) images of parasites grown under IR (0 μM) and HI (250 μM) conditions; nuclei stained with DAPI (in blue; b, g, l and q); parasites labelled with DIL (in red; c, h, m and r) as a membrane marker; TvCP2 (labelled with FITC; in green; d, i, n and s) staining of parasites incubated with the anti-TvCP2r antibody (1:100 dilution) and a FITC-conjugated secondary antibody (1:100 dilution); merge of the co-localization of TvCP2 with membrane marker (in yellow; e, j, o and t). Preimmune (PI) serum was used as a negative control representative of all experiments (panels u–y), using non-permeabilized parasites. The slides were observed at 63× magnification by confocal microscopy (Zeiss) 3D maximum projection. Scale bar = 10 μM. (C) Localization of TvCP2 in lysosomes was performed using parasites incubated with Lysotracker (in red; c and h), fixed and permeabilized with Triton X-100 and incubated with the anti-TvCP2r antibody as in (B) (in green; d and i) (merge; e and j). The scant co-localization of TvCP2 with lysosomes (in yellow; e). Nuclei were stained with DAPI (in blue; b and g). The slides were observed at 63× magnification by confocal microscopy (Zeiss) 3D maximum projection. Differential phase contrast (DPC; a and f) images of parasites grown under IR and HI conditions. Scale bar = 10 μM.

with the membrane marker DIL (in red) with a Pearson's correlation coefficient of $r = 0.76$ (Fig. 3A, panels e and j), supporting a surface localization of TvCP2. TvCP2 was also detected in cytoplasmic spots in permeabilized parasites that could correspond to lysosomes and/or secretory vesicles (Fig. 3B, panels n, o, s and t). The PI serum exhibited no reaction (Fig. 3B). To corroborate whether TvCP2 may also have a lysosomal localization in the parasite, an assay using live parasites incubated with Lysotracker Red before IFA with the anti-TvCP2r antibody

(in green) was performed. Figure 3C shows the presence of lysosomes (in red; panels c and h). However, the co-localization of both labels was observed only in few spots (in yellow; panel e), suggesting that TvCP2 may also be present in some lysosomes. Nevertheless, the co-localization analysis reported a Pearson's correlation coefficient of $r = 0.46$, suggesting a minor lysosomal localization of TvCP2 (Fig. 3C, panels e and j). Thus, some of the TvCP2 spots could correspond to secretory vacuoles.

TvCP2 could be a protease targeted by TC-3

We recently determined that an endogenous CP inhibitor, trichocystatin 3 (TC-3), interacts with and inhibits the proteolytic activity of several trichomonad CPs, thereby reducing cellular damage (Sánchez-Rodríguez *et al.*, 2018). We aimed to evaluate whether TvCP2 is another CP target for TC-3 using a similar approach. Thus, a pull-down assay was performed as reported by Sánchez-Rodríguez *et al.* (2018) using TC-3r as bait protein and trichomonad extract as a source of TvCP2. The TC-3r-bound proteins were eluted and analysed by SDS-PAGE and WB assays. An eluted 30 kDa very weak protein band was detected in CBB-stained gels. Besides, a prominent 14.2 kDa protein band that corresponds to TC-3r, used as an anchor, was also eluted (Fig. 4A, lane 2). Finally, to detect whether the TvCP2 protease was present in the eluted fraction, we performed a WB assay using the anti-TvCP2r antibody and an anti-TvTIMr antibody (Miranda-Ozuna *et al.*, 2016) and PI serum as negative controls. The eluted TC-3r pull-down and CPE showed the presence of the ~27 kDa TvCP2 band that corresponds to the molecular mass of the mature protease (Fig. 4B). As expected, neither the PI serum nor the anti-TvTIMr antibody used as negative controls showed any recognition in the eluted fraction from the TC-3 pull-down assay. Similarly, the anti-TvTIMr antibody detected a protein band only in the control CPE. The HSP70r and BSA proteins were used as control bait proteins (as an unrelated and negative control protein, respectively; Figure 4A). The HSP70r pull-down assay showed very weak protein bands at ~56–65 kDa in the CBB-stained gel (Fig. 4A). However, the WB did not show recognition by the anti-TvCP2r antibody (Fig. 4B). Similarly, the BSA pull-down assay did not show any band in the gel (Fig. 4A), and by WB, there was no recognition (Fig. 4B), showing that the TC-3r/TvCP2 interaction was specific. These data show that TvCP2 could be one of the CPs targeted by TC-3 *in T. vaginalis*.

Limited co-localization of TC-3 with TvCP2 in T. vaginalis

To verify whether the binding of the TC-3 inhibitor with TvCP2 identified by pull-down and WB assays occurs in the same cellular compartment of *T. vaginalis*, co-localization of IFA of TC-3 with TvCP2 were performed. First, we determined the localization of TvCP2 in non-permeabilized CNCD280 Tv isolate (a type 1 isolate). The TvCP2 protease (Fig. 4C, panel c; green label) was detected on the plasma membrane (Fig. 4C, panel b; red label) as prominent spots in non-permeabilized parasites (Fig. 4C, panel d; yellow label). The negative control did not show any green label, as expected (Fig. 4C, panels g and h). In permeabilized Tv, immunofluorescence showed a punctate pattern of TvCP2 distribution throughout the cell, compatible with vesicular localization (Fig. 4D, panel b; red label) consistent with ultrastructural data (Fig. 4E, panels b–e). The subcellular localization of TvCP2 in the whole parasite is shown as a specificity control (Fig. 4E, panel b). TvCP2 accumulates mainly in vesicles and close to the parasite surface. The negative control did not show any gold particles, as expected (Fig. 4E, panel a). Figure 4D immunofluorescence merge images revealed limited co-localization of TvCP2 (panel b, red label) and TC-3 (panel c, green label) at both in an area close to the nucleus and in some puncta (panel d, yellow label, white arrowheads). The organelles where TvCP2 and TC-3 may co-localize were subsequently identified by immune gold labelling as in vesicles and on the parasite surface by electron microscopy (TEM; Figure 4F), but the frequency of co-localization was minimal. For example, TvCP2 was frequently observed in TC-3-free vesicles and TC-3 in TvCP2-free vesicles (Fig. 4F, panel e). Although both molecules were also found in the organelle – Golgi complex – these were

not in close proximity (Fig. 4F, panel f), suggesting that these two molecules do not interact in the Golgi complex either; instead, both molecules may undergo glycosylation and follow the classical secretory pathway. Occasionally, the TvCP2 and TC-3 molecules were observed in close proximity (Fig. 4F, panels g–i) in some vesicles and on the parasite surface. The negative control did not show any gold particles (Fig. 4F, panels a–d). Thus, these data suggest that the TvCP2 protease has a limited interaction with TC-3 at these parasite compartments (vacuoles and parasite surface). Thus, our data could not confirm the co-localization of TvCP2 with TC-3 in the parasite. However, these results could also suggest the TvCP2 is not the main CP targeted by TC-3, but could also suggest that TvCP2 may be interacting with any of the two trichocystatin inhibitors of trichomonads, such as TC-1 or TC-2 (Carlton *et al.*, 2007).

TvCP2 plays a key role in trichomonal cytotoxicity and apoptosis induction in HeLa cell monolayers

To investigate the role of TvCP2 on trichomonal cytotoxicity under the influence of iron, the effect of iron on the levels of trichomonal cytotoxicity in HeLa cell monolayers was first examined. Parasites grown under IR conditions were more cytotoxic than those grown under HI conditions (Fig. 5A). To determine whether TvCP2 is involved in trichomonal cytotoxicity towards HeLa cell monolayers modulated by IR conditions, live IR parasites were pretreated with increasing concentrations (0–300 μg mL^{-1}) of purified anti-TvCP2r IgGs or with PI serum IgGs used as a negative control. The anti-TvCP2r antibody showed a protective effect on HeLa cell monolayers by reducing cytotoxicity levels by up to 40% (Fig. 5B). The PI serum-pretreated parasites destroyed the HeLa cell monolayers as the untreated parasites did. These data showed that the interaction of live parasites with the anti-TvCP2 antibody reduced the TvCP2-dependent trichomonal cytotoxicity under IR conditions.

To further confirm the role played by TvCP2 in the HeLa cell damage triggered by *T. vaginalis*, three different apoptosis inhibition assays were performed. Two of them, through DNA fragmentation assays assessed by a TUNEL assay and by DNA laddering observed by agarose gel electrophoresis using the highest concentration of anti-TvCP2 IgGs in the cytotoxicity inhibition assays (Fig. 5B). Figure 5C and D and Supplementary Fig. S5 (lanes 1 and 4) show the lack of TUNEL reaction (no green label) and the control of high molecular size bands, respectively, that correspond to HeLa cells and trichomonad genomic DNA, as indicative of DNA integrity before the host–parasite interaction. The induction of apoptosis (as a positive control of DNA degradation) was achieved by the treatment of both cell types with 5% H$_2$O$_2$ for 30 and 60 min at 37°C (Singh *et al.*, 2007) and the fragmentation/degradation of both genomic DNAs was observed. In HeLa cells and trichomonads after H$_2$O$_2$ treatment, DNA fragmentation was observed as a TUNEL-positive reaction (green label; Supplementary Fig. S4). These results were supported by the DNA degradation observed in the agarose gel as a reduction of the genomic DNA band and as smears mainly in the Tv gDNA (Supplementary Fig. S5, lanes 2, 3, 5, 6). Analysis of the genomic DNA after parasite–host cell interaction showed DNA fragmentation detected by a TUNEL positive reaction (green label; Fig. 5C and D) and DNA degradation detected by a reduction of the high molecular size DNA band and an enrichment of a lower size DNA band (Supplementary Fig. S5, lane 7) compared with the control DNAs (Supplementary Fig. S5, lanes 1 and 4). However, after the interaction of anti-TvCP2r IgG-pretreated parasites with HeLa cell monolayers, the lack of TUNEL reaction (no green label; Fig. 5C and D) and a certain degree of protection of the
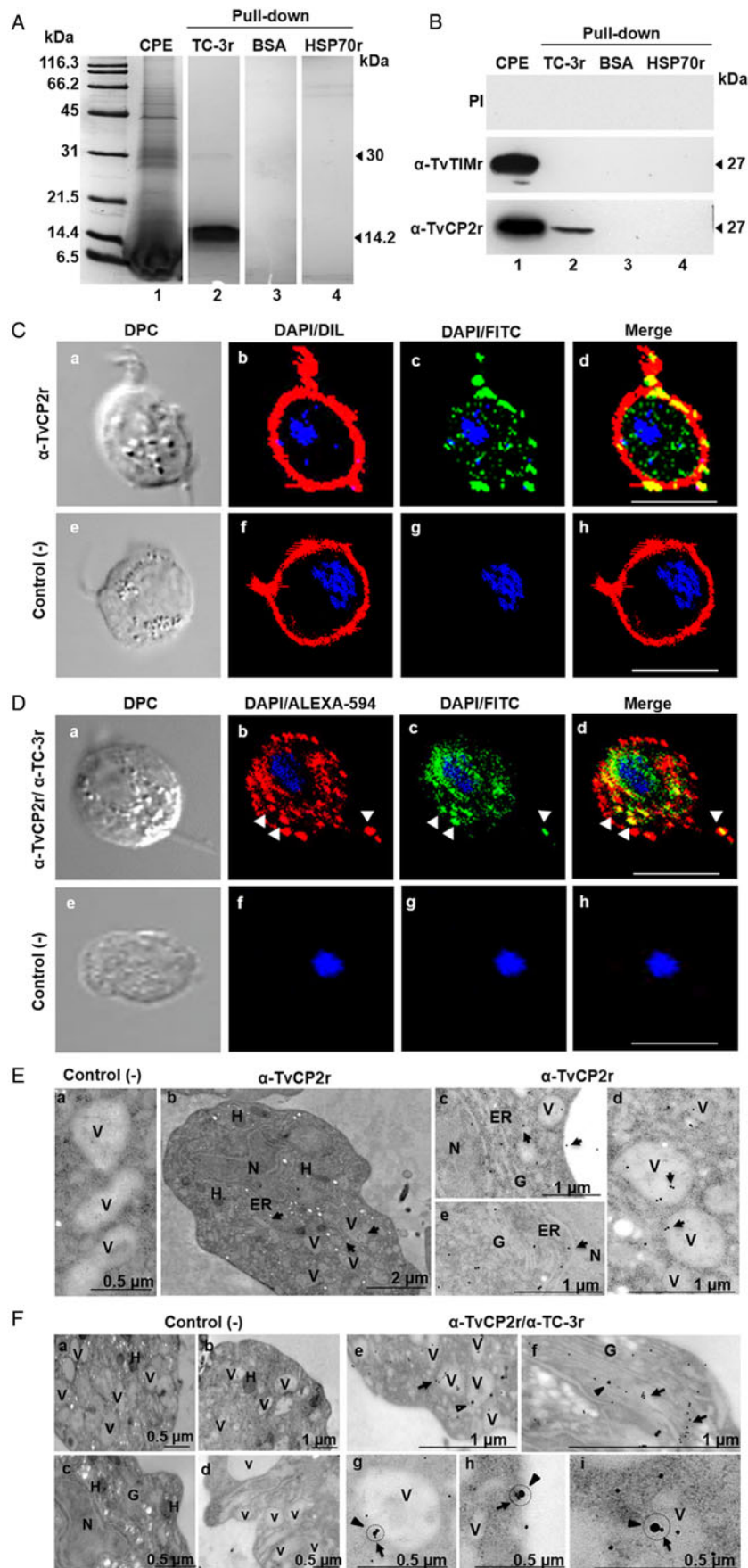
Fig. 4. TvCP2 could be targeted by TC-3r in *T. vaginalis*. (A) Pull-down assay with TC-3r; CBB-stained gel. Lane 1, a clarified protein extract (CPE) from the CNCD280 Tv isolate; lane 2, elution fraction using TC-3r as bait protein; lanes 3–4, elution fractions using BSA or HSP70r as control bait proteins, respectively. (B) Western-blot assay using duplicate samples from (A). Lane 1, CPE; lanes 2–4, elution fractions after a pull-down assay with TC-3r, BSA and HSP70r, respectively. For WB, the following antibodies were tested: PI serum, anti-TvTIMr and anti-TvCP2r. (C) Confocal microscopy analysis of TvCP2 localization using a rabbit anti-TvCP2r antibody, a preimmune serum used as a negative control, and a FITC-labelled secondary antibody (in green; panels c, d, g and h), DIL (panels b, d, f and h; in red) as a membrane marker, and DAPI (panels b–d; panels f–h; in blue) as a nucleus marker. Merged (panels d and h) and DPC (panels a and e). (D) Co-localization analysis by indirect immunofluorescence assays and confocal microscopy using rabbit anti-TvCP2r and mouse anti-TC-3r as primary antibodies. Alexa Fluor-594-labelled (in red, panels b, d, f and h) secondary antibody for TvCP2 and FITC-labelled secondary antibody for TC-3 (in green, panels c, g, d and h). Merged (panels d and h) and DPC (panels a and e). White arrowheads point to discrete areas of each label alone (panels b and c) and in co-localization (yellow label; panel d). The slides were observed at 63× magnification by confocal microscopy (Zeiss). Scale bar = $10\,\mu$M. (E) TEM immunogold labelling with a rabbit anti-TvCP2r antibody and a 20 nm gold particle secondary antibody. Panel a, the secondary antibody alone was used as a negative control (−) for TEM immunolocalization assays. Panel b shows the subcellular localization of TvCP2 in the whole parasite, as a specificity control. Panels c–e show localization of TvCP2 in the ER, near the Golgi complex and vacuoles. (F) Co-localization by TEM with immunogold labelling for mouse anti-TC-3r (30 nm particle) and rabbit anti-TvCP2r (15 nm particle) as primary antibodies were analysed according to the method described by Pastorek *et al.* (2016). Panels a–d are images using both secondary antibodies alone as negative controls for TEM immunoco-localization assays. Panel e shows localization of TvCP2 in TC-3-free vacuoles and of TC-3 in TvCP2-free vacuoles. Panel f shows localization of both molecules in the Golgi complex, but not in close proximity. Panels g–i (black circle) show co-localization (close proximity) of TC-3 and TvCP2 labels on the vacuole membrane and on the plasma membrane. Subcellular compartments observed in panels E and F by TEM: N, nucleus; H, hydrogenosome; V, vacuoles; ER, endoplasmic reticulum, G, Golgi complex; black arrow in Fig. 4E, panel c indicates plasma membrane; black circles in Fig. 4F, panels g–i indicate co-localization between TC-3 and TvCP2. Black arrows in Fig. 4E, panels b–e and Fig. 4F, panels e–i indicate the compartments where the TvCP2 label is concentrated. Black arrowheads in Fig. 4F panels e–i indicate the compartments where the TC-3 label is observed.

genomic DNA integrity was observed (Supplementary Fig. S5, lane 9) compared with the interactions with PI serum IgG-pretreated parasites (Fig. 5C and D; Supplementary Fig. S5, lane 8) used as a control.

Additionally, an apoptosis inhibition assay followed by the Annexin V-FITC method in the presence of the anti-TvCP2r or PI serum IgGs was performed. Apoptosis induction in HeLa cell monolayers by IR parasites (used as a positive control) showed a
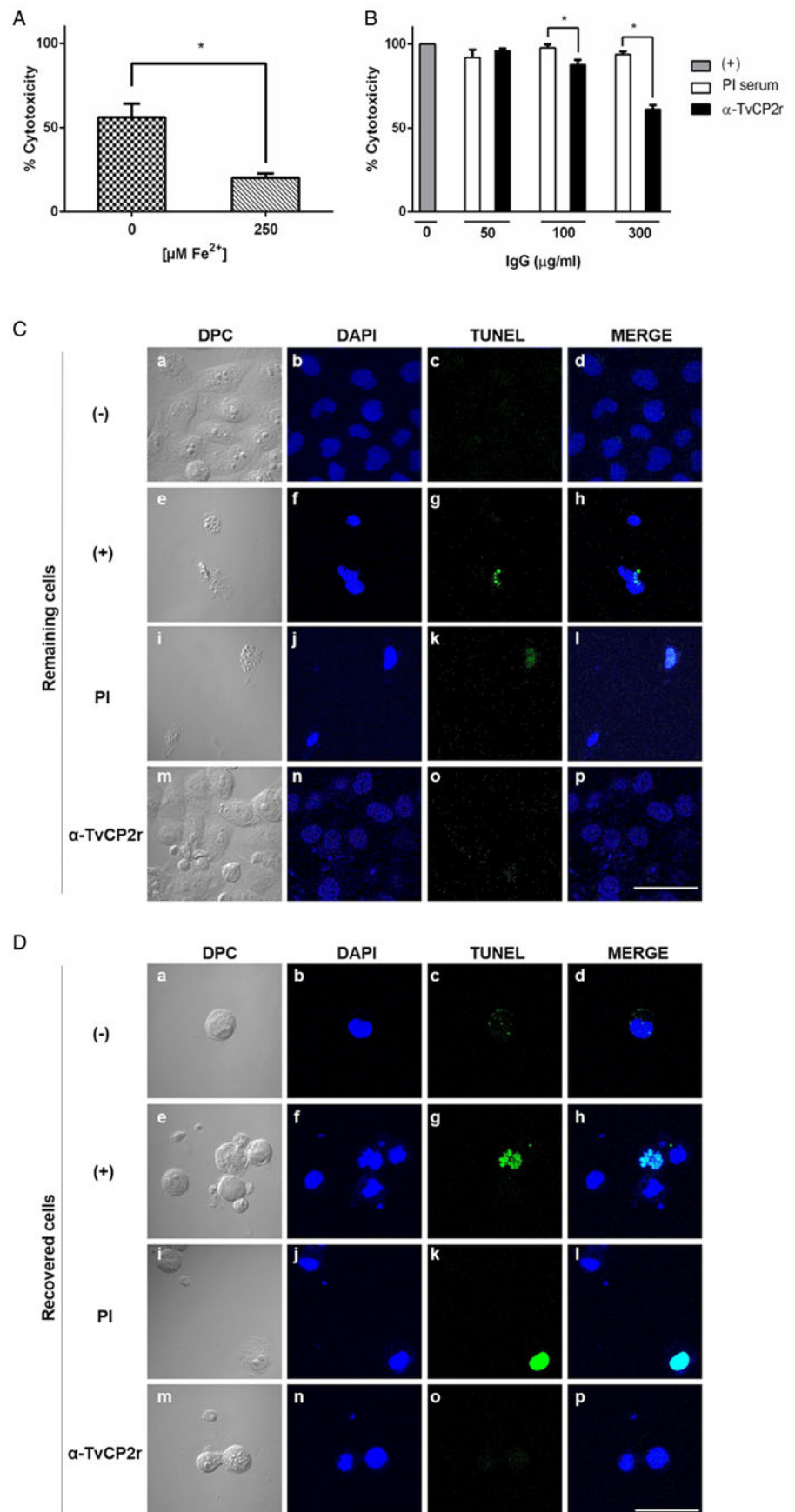
Fig. 5. TvCP2 participates in cellular damage to HeLa cells through apoptosis induction detected as DNA fragmentation by TUNEL assay. (A) Cytotoxicity assays were performed using 2×10^5 live parasites grown under IR ($0\,\mu$M) and HI ($250\,\mu$M) conditions. (B) Cytotoxicity inhibition assays were done using 2×10^5 live parasites grown under IR conditions and pretreated with increasing concentrations of purified IgGs of the anti-TvCP2r antibody or preimmune (PI) serum, followed by interaction with HeLa cell monolayers (3.5×10^4 well^{-1}). As a negative control (−), HeLa cell monolayers without parasites were used. As a positive control (+), HeLa cell monolayers with parasites grown under IR conditions without antibody pretreatment were used, and their level of destruction was set as 100% cytotoxicity. Each point in the bar represents the mean of the percentage of the destruction of the HeLa cell monolayer for representative experiments with triplicate samples (panel B). (C and D) TUNEL assay was performed after the interaction of HeLa cells with trichomonads as previously described in (B). Inhibition of apoptosis induction detected by TUNEL was performed with live parasites pretreated with $300\,\mu$g ml^{-1} of anti-TvCP2 purified IgGs. Parasites pretreated with the same amount of IgGs purified from preimmune (PI) serum were used as a negative control for the inhibition assays. HeLa cell monolayer without treatment was used as a negative control. HeLa cell monolayers incubated with live parasites were used as a positive control. After the interaction, the remaining cells attached to the coverslips (C) and released into the culture medium (D) were incubated with TdT transferase and the fluorescein-labelled nucleotide mix, as recommended by the manufacturer, and observed by confocal microscopy (Zeiss). (C and D) Differential Phase Contrast (DPC; panels a, e, I and m), DAPI (in blue, panels b, f, j and n), fluorescent TUNEL label (in green, panels c, g, k and o) and merge (panels d, h, l and p). These experiments were performed at least two independent times with similar results. The slides were observed at 63× magnification by confocal microscopy (Zeiss) 3D maximum projection. Scale bar = $20\,\mu$M.

strong Annexin V (in green) fluorescence intensity and extensive cytotoxic damage of HeLa cell monolayers compared to the lack of Annexin V fluorescent signal in the negative control of HeLa cell monolayers (Supplementary Fig. S6A). The cytotoxic damage of the HeLa cell monolayer and the fluorescence intensity of Annexin V were reduced (up to 46.6 ± 2.2%) by the anti-TvCP2r IgGs, but not by the PI serum IgG (81 ± 11.1%) (Supplementary Fig. S6B) and these differences were significant ($P < 0.05$).

Thus, all together these data support the participation of TvCP2 in trichomonal cytotoxicity due to apoptosis induction as a cell death mechanism in HeLa cell monolayers, as previously suggested (Sommer *et al.*, 2005; Kummer *et al.*, 2008) that occurred in parasite grown under different starvation conditions such as putrescine (Carvajal-Gámez *et al.*, 2014), zinc (Puente-Rivera *et al.*, 2017), glucose (Miranda-Ozuna *et al.*, 2019) and iron, as shown in this work.

Discussion

Iron is an essential nutrient for *T. vaginalis*. Similar to other amitochondriate protozoa, such as *E. histolytica* and *Giardia lamblia*, iron is necessary for high amounts (50–300 μM) for parasite metabolism, multiplication and survival that results in competition for iron between the pathogen and host during the infection (Lehker and Alderete, 1992; Ortíz-Estrada *et al.*, 2015). Like glucose, the scarcity of iron is a metabolic stress that induces the activation of survival mechanisms and acts as a regulator of virulence factors such as CPs and other metabolic enzymes (Figueroa-Angulo *et al.*, 2012; Arroyo *et al.*, 2015). Also, an iron-responsive promoter-dependent transcriptional iron regulatory mechanism and an iron-responsive element/iron regulatory protein-like (IRE/IRP-like) system that participate in a post-transcriptional mechanism mediated by iron have been identified in this parasite (Tsai *et al.*, 2002; Solano-González *et al.*, 2007; Torres-Romero and Arroyo, 2009; Figueroa-Angulo *et al.*, 2015), indicating that fluctuations in iron concentrations also play a crucial role in the regulation of gene expression in *T. vaginalis*, as previously shown at the transcriptomic level (Horváthová *et al.*, 2012).

Trichomonas vaginalis is a parasitic protozoan with a complex active degradome due to its high proteolytic activity that includes the activities of cathepsin-L-like and legumain-like CPs (Ramón-Luing *et al.*, 2010). Some of these CPs were identified as part of the trichomonad immunoproteome detected by trichomoniasis patient sera (TvCP2, TvCP4, TvCP39) (Ramón-Luing *et al.*, 2010), suggesting their presence and participation during infection in the host–parasite interaction (CP30 and TvCP39) (Sommer *et al.*, 2005; Kummer *et al.*, 2008; Ramón-Luing *et al.*, 2011). However, the role of some of these CPs, such as TvCP2, during infection has not been characterized.

Thus, the goals of this work were as follows: (1) to demonstrate that TvCP2 is immunogenic and that is present in vaginal secretions of patients with trichomoniasis, as a meaning of its expression during infection and (2) to assess the effect of iron on TvCP2 expression, localization and participation in trichomonal cytotoxicity. In this work, we demonstrated the presence of TvCP2 in vaginal secretions, confirmed its immunogenicity and suggested that TvCP2 could be a protease targeted by the TC-3 inhibitor, which could regulate its proteolytic activity at the post-translational level, as has been reported for TC-2 and TvCP39 (Puente-Rivera *et al.*, 2014). Further, the effect of iron on the expression and localization of TvCP2 and its role in cellular damage was determined.

Our results demonstrated that TvCP2 protein is expressed, processed to the mature form and triggers an immunological response in Tv-infected people, since anti-TvCP2 antibodies were found in sera from Tv (+) patients (Fig. 1B). These data are consistent with the Tv immunoproteome analysis (Ramón-Luing *et al.*, 2010), suggesting that TvCP2 could be a putative biomarker of trichomoniasis. TvCP2 is also released during trichomonal infection as the mature form, since a 27 kDa TvCP2 protein band was found in vaginal fluids from Tv (+) patients (Fig. 1C; Supplementary Fig. S1B). These results are consistent with previous reports that showed active *in vitro* and *in vivo* secretion of CPs by the parasite and the presence of some trichomonad CPs of the 30 kDa region in vaginal secretions (Neale and Alderete, 1990; Mendoza-López *et al.*, 2000; Hernández-Gutiérrez *et al.*, 2003, 2004; Ramón-Luing *et al.*, 2011). Moreover, mature TvCP2 is released in SPs by metabolically active parasites under different iron conditions *in vitro* (Fig. 2G).

Our results also suggest a possible vesicular secretory pathway for the secretion of TvCP2 since TvCP2 shows cytoplasmic vacuolar localization that most of them do not correspond to lysosomes (Fig. 3). Thus, the punctate fluorescent staining could correspond to autophagy or secretion vesicles that follow a secretory pathway to reach the parasite membrane and subsequent secretion. However, the secretion pathway of TvCP2 is still unknown. Further studies are necessary to elucidate the TvCP2 secretory pathway. Thus, the presence of TvCP2 in Tv (+) VWs (Fig. 1) could be due to active secretion during infection that occurs under different iron conditions (Fig. 2), as well as under glucose starvation, as we recently described (Miranda-Ozuna *et al.*, 2019), suggesting that several host components could regulate trichomonad gene expression, in particular TvCP2 and other CPs, which may be closely regulated by fluctuations in iron and glucose concentrations during the menstrual cycle (Figueroa-Angulo *et al.*, 2012; Miranda-Ozuna *et al.*, 2019). These responses allow the parasite to adapt to the changing environment and survive during periods of nutrient scarcity in the host to maintain the infection (Torres-Romero and Arroyo, 2009). These results are consistent with previous reports on the analysis of the Tv immunoproteome, in which TvCP2 was one of the spots detected by Tv (+) patient sera (Ramón-Luing *et al.*, 2010), rendering it as a putative biomarker for immunodiagnosis.

Additionally, TvCP2 was downregulated by iron at the mRNA and protein levels, in its localization (Figs 2 and 3), and at the functional level. Furthermore, iron also played an important role in trichomonal cytotoxicity through apoptosis induction in HeLa cell monolayers under IR conditions (Fig. 5; Supplementary Figs S4–S6). These results are consistent with previous reports (Sommer *et al.*, 2005; Kummer *et al.*, 2008) and like the previously reported iron downregulation of TvCP12 and TvCP65 at the transcript and protein levels. These CPs also participate in cellular destruction (León-Sicairos *et al.*, 2004; Alvarez-Sánchez *et al.*, 2007; our unpublished results). However, it is interesting to notice that TvCP2 is one of the molecules downregulated by iron and, despite that, participates in cellular damage. These data are contrasting with those previously reported by Ryu *et al.* (2001), in which cytotoxicity increased under high iron conditions and during menstruation. However, it is important to notice that the parasite activates some CPs under nutrient starvation. The parasite became more aggressive under iron restriction to be able to acquire iron from epithelial cells. Indeed, our results showed that it is under IR microenvironmental conditions when TvCP2 participates in cellular damage mediated by apoptosis induction. These results are consistent with those previously reported by Kummer *et al.* (2008), in which TvCP2 is part of the CP30 *in vitro* secretory products from parasites under IR conditions.

Moreover, the *tvcp2* iron-mediated downregulation shown in our work (Fig. 2A) is consistent with the transcriptomic analysis reported in parasites under IR and HI conditions (Horváthová *et al.*, 2012). However, the mechanism underlying the iron-mediated downregulation of *tvcp2* gene expression remains unknown. Thus, it is important to elucidate how the iron regulatory mechanism occurs, which may help to understand the adaptation and pathogenicity of the parasite under nutrient starvation in the vaginal microenvironment during the menstrual cycle.

Interestingly, regulation of TvCP2-active cytotoxic activity may be carried out, in part by TC-3, a surface endogenous CP

inhibitor of TvCP2, which has been shown to inhibit several CPs (Sánchez-Rodríguez *et al.*, 2018). Indeed, pull-down assays showed the interaction of TC-3r and TvCP2 (Fig. 4A and B) and co-localization assays by IFA and immunogold localization by TEM (Fig. 4D and F) showed the presence of limited co-localization events of TC-3r and TvCP2 in cytoplasm vacuoles, and on the parasite surface (Fig. 4F, panels g–i), which may also help to control the contribution of TvCP2 to cellular damage. Nevertheless, the co-localization detected between both molecules was limited and insufficient to support a putative interaction detected by using immunoco-localization assays, as described here (Fig. 4D and F). This could be because the parasite requires the protease in an active form and not tightly regulated in these cellular compartments. Moreover, TvCP2 could not be the main protease targeted by TC-3 inhibitor, or that TvCP2 protease is associated with another trichomonad CP inhibitor, as was previously reported for TvCP39 and TC-2 (Puente-Rivera *et al.*, 2014). Further studies will help to elucidate the nature of the molecular and biological interaction between these molecules of *T. vaginalis*. These data did show that TvCP2 localization was similar in the two types of Tv isolates used here (Conrad *et al.*, 2012).

Moreover, the participation of TC-3 in modulating the trichomonal cytotoxicity effect on HeLa cell monolayers (Sánchez-Rodríguez *et al.*, 2018) shows that TC-3r exhibits inhibitory activity over certain cytotoxic CPs located on the parasite surface and plays a role in the post-translational regulation of this virulence property (Alvarez-Sánchez *et al.*, 2000, 2007; Hernández-Gutiérrez *et al.*, 2003, 2004; Ramón-Luing *et al.*, 2011; Arroyo *et al.*, 2015). Our results then support the participation of TvCP2 that together with TvCP39, TvCP12, TvCP65 and TvCP3 in trichomonal cytotoxicity, since the TC-3/CP interaction occurs on the parasite surface (Sánchez-Rodríguez *et al.*, 2018), which is similar to the interaction of these cytotoxic CPs with TC-2r, another endogenous CP inhibitor of *T. vaginalis* (Puente-Rivera *et al.*, 2014).

The results obtained in this work regarding the cytotoxicity and apoptosis inhibition assays using the anti-TvCP2r antibody confirmed that TvCP2 is used by trichomonads to induce cellular destruction, damage to DNA and cell death of the HeLa cell monolayers also under iron starvation conditions (Fig. 5; Supplementary Figs S4–S6). However, Tv cellular damage under IR conditions is not as drastic as the monolayer destruction observed using parasites cultured under glucose-restricted conditions (Miranda-Ozuna *et al.*, 2019), suggesting that the effect of iron starvation differentially regulates the participation and the effect of the distinct trichomonal factors involved in the cytotoxic mechanisms, such as porins, phospholipase A, a cell detaching factor (Petrin *et al.*, 1998; Fiori *et al.*, 1999; Lubick and Burgess, 2004). Thus, further studies are necessary to elucidate the mechanisms of apoptosis induction by TvCP2 related to iron and glucose starvation.

In conclusion, in this study, we determined that iron downregulates TvCP2, a cysteine protease present in vaginal secretions from patients with active infection. This *T. vaginalis* protease plays a key role in trichomonal cytotoxicity by the induction of apoptosis in HeLa cell monolayers. Additionally, TvCP2 could also be post-translationally regulated by TC-3, a surface endogenous CP inhibitor in this protist parasite.

References

Adler J and Parmryd I (2010) Quantifying colocalization by correlation: the Pearson correlation coefficient is superior to the Mander's overlap coefficient. *Cytometry Part A*, **77**, 732–742. doi: 10.1002/cyto.a.20896.

Alderete JF, Provenzano D and Lehker MW (1995) Iron mediates *Trichomonas vaginalis* resistance to complement lysis. *Microbial Pathogens* **19**, 93–103.

Alvarez-Sánchez ME, Ávila-González L, Becerril-García C, Fattel-Facenda LV, Ortega-López J and Arroyo R (2000) A novel cysteine proteinase (CP65) of *Trichomonas vaginalis* involved in cytotoxicity. *Microbial Pathogens* **28**, 193–202.

Alvarez-Sánchez ME, Solano-González E, Yáñez-Gómez C and Arroyo R (2007) Negative iron regulation of the CP65 cysteine proteinase cytotoxicity in *Trichomonas vaginalis*. *Microbes and Infection* **9**, 1597–1605.

Arroyo R and Alderete JF (1989) *Trichomonas vaginalis* surface proteinase activity is necessary for adherence to epithelial cells. *Infection and Immunity* **57**, 2991–2997.

Arroyo R and Alderete JF (1995) Two *Trichomonas vaginalis* surface proteinases bind to host epithelial cells and are related to levels of cytoadherence and cytotoxicity. *Archives of Medical Research* **26**, 279–285.

Arroyo R, Cárdenas-Guerra RE, Figueroa-Angulo EE, Puente-Rivera J, Zamudio-Prieto O and Ortega-López J (2015) *Trichomonas vaginalis* cysteine proteinases: iron response in gene expression and proteolytic activity. *Biomed Research International* **2015**, 946787. doi: 10.1155/2015/946787.

Benchimol M (2004) Trichomonads under microscopy. *Microscopy and Microanalysis* **10**, 528–550.

Cárdenas-Guerra RE, Arroyo R, Rosa de Andrade I, Benchimol M and Ortega-López J (2013) The iron-induced cysteine proteinase TvCP4 plays a key role in *Trichomonas vaginalis* haemolysis. *Microbes and Infection* **15**, 958–968.

Cárdenas-Guerra RE, Ortega-López J, Flores-Pucheta CI, Benítez-Cardoza CG and Arroyo R (2015) The recombinant prepro region of TvCP4 is an inhibitor of cathepsin L-like cysteine proteinases of *Trichomonas vaginalis* that inhibits trichomonal haemolysis. *International Journal of Biochemistry and Cell Biology* **59**, 73–83.

Carlton JM, Hirt RP, Silva JC, Delcher AL, Schatz M, Zhao Q, Wortman JR, Bidwell SL, Alsmark UC, Besteiro S, Sicheritz-Ponten T, Noel CJ, Dacks JB, Foster PG, Simillion C, Van de Peer Y, Miranda-Saavedra D, Barton GJ, Westrop GD, Müller S, Dessi D, Fiori PL, Ren Q, Paulsen I, Zhang H, Bastida-Corcuera FD, Simoes-Barbosa A, Brown MT, Hayes RD, Mukherjee M, Okumura CY, Schneider R, Smith AJ, Vanacova S, Villalvazo M, Haas BJ, Pertea M, Feldblyum TV, Utterback TR, Shu CL, Osoegawa K, de Jong PJ, Hrdy I, Horvathova L, Zubacova Z, Dolezal P, Malik SB, Logsdon JM Jr, Henze K, Gupta A, Wang CC, Dunne RL, Upcroft JA, Upcroft P, White O, Salzberg SL, Tang P, Chiu CH, Lee YS, Embley TM, Coombs GH, Mottram JC, Tachezy J, Fraser-Liggett CM and Johnson PJ (2007) Draft genome sequence of the sexually transmitted pathogen *Trichomonas vaginalis*. *Science (New York, N.Y.)* **315**, 207–212.

Carvajal-Gámez BI, Quintas-Granados LI, Arroyo R, Vázquez-Carrillo LI, Ramón-Luing LL, Carrillo-Tapia E and Álvarez-Sánchez ME (2014) Putrescine-dependent re-localization of TvCP39, a cysteine proteinase involved in *Trichomonas vaginalis* cytotoxicity. *PLoS ONE* **9**, e107293.

Conrad MD, Gorman AW, Schillinger JA, Fiori PL, Arroyo R, Malla N, Dubey ML, González J, Blank S, Secor WE and Carlton JM (2012) Extensive genetic diversity, unique population structure and evidence of genetic exchange in the sexually transmitted parasite *Trichomonas vaginalis*. *PLoS Neglected Tropical Diseases* **6**, e1573.

Dailey DC, Chang TH and Alderete JF (1990) Characterization of *Trichomonas vaginalis* haemolysis. *Parasitology* **101**, 171–175.

De Jesus JB, Ferreira MA, Cuervo P, Britto C, Silva-Filho FC and Meyer-Fernandes JR (2006) Iron modulates ecto-phosphohydrolase activities in pathogenic trichomonads. *Parasitoloy Internacional* **55**, 285–290.

De Jesus JB, Cuervo P, Junqueira M, Britto C, Silva-Filho FC, Soares MJ, Cupolillo E, Fernandes O and Domont GB (2007) A further proteomic study on the effect of iron in the human pathogen *Trichomonas vaginalis*. *Proteomics* **7**, 1961–1972.

Diamond LS (1957) The establishment of various trichomonads of animals and man in axenic cultures. *Journal of Parasitology* **43**, 488–490.

Dias-Lopes G, Saboia-Vahia L, Margotti ET, Fernandes NS, Castro CLF, Oliveira FO, Peixoto JF, Britto C, Silva-Filho FCE, Cuervo P and Jesus JB (2017) Morphologic study of the effect of iron on pseudocysts formation un *Trichomonas vaginalis* and its interaction with human epithelial cells. *Memórias do Instituto Oswaldo Cruz* **112**, 664–673.

Figueroa-Angulo EE, Rendón-Gandarilla FJ, Puente-Rivera J, Calla-Choque JS, Cárdenas-Guerra RE, Ortega-López J, Quintas-Granados LI, Álvarez-Sánchez ME and Arroyo R (2012) The effects of environmental factors on the virulence of *Trichomonas vaginalis*. *Microbes and Infection* **14**, 1411–1427.

Fiori PL, Rappelli P, Rocchigiani AM and Cappuccinelli P (1993) *Trichomonas vaginalis* haemolysis: evidence of functional pores formation on red cell membranes. *FEMS Microbiology* **109**, 13–18.

Fiori PL, Rappelli P, Addis MF, Sechi A and Capuccinelli P (1996) *Trichomonas vaginalis* haemolysis: pH regulates a contact-independent mechanism based on pore-forming proteins. *Microbial Pathogens* **20**, 109–118.

Fiori PL, Rappelli P and Addis MF (1999) The flagellated parasite *Trichomonas vaginalis*: new insights into cytopathogenicity mechanisms. *Microbes and Infection* **1**, 149–156.

Gorrell TE (1985) Effect of culture medium iron content on the biochemical composition and metabolism of *Trichomonas vaginalis*. *Journal of Bacteriology* **161**, 1228–1230.

Harlow E and Lane D (1988) *Antibodies: A Laboratory Manual*. New York: Cold Spring Harbor Laboratory, pp. 298–300. ISBN 0-87969-314-2.

Hernández-Gutiérrez R, Ortega-López J and Arroyo R (2003) A 39-kDa cysteine proteinase CP39 from *Trichomonas vaginalis*, which is negatively affected by iron may be involved in trichomonal cytotoxicity. *Journal of Eukaryotic Microbiology* **50**(Suppl), 696–698.

Hernández-Gutiérrez R, Avila González L, Ortega-López J, Cruz-Talonia F, Gómez-Gutiérrez G and Arroyo R (2004) *Trichomonas vaginalis*: characterization of a 39-kDa cysteine proteinase found in patient vaginal secretions. *Experimental Parasitology* **107**, 125–135.

Hernández HM, Marcet R and Sarracent J (2014) Biological roles of cysteine proteinases in the pathogenesis of *Trichomonas vaginalis*. *Parasite* **21**, 54.

Horváthová L, Šafaríková L, Basler M, Hrdy I, Campo NB, Shin JW, Huang KY, Huang PJ, Lin R, Tang P and Tachezy J (2012) Transcriptomic identification of iron-regulated and iron-independent gene copies within the heavily duplicated *Trichomonas vaginalis* genome. *Genome Biological Evolution* **4**, 1017–1029.

Kummer S, Hayes GR, Gilbert RO, Beach DH, Lucas JJ and Singh BN (2008) Induction of human host cell apoptosis by *Trichomonas vaginalis* cysteine proteases is modulated by parasite exposure to iron. *Microbial Pathogens* **44**, 197–203.

Lehker MW and Alderete JF (1992) Iron regulates growth of *Trichomonas vaginalis* and the expression of immunogenic trichomonad proteins. *Molecular Microbiology* **6**, 123–132.

Lehker MW and Alderete JF (2000) Biology of trichomonosis. *Current Opinion in Infectious Diseases* **13**, 7–45.

León-Sicairos CR, León-Félix J and Arroyo R (2004) Tvcp12: a novel *Trichomonas vaginalis* cathepsin L-like cysteine proteinase encoding-gene. *Microbiology (Reading, England)* **150**, 1131–1138.

Lubick KJ and Burgess DE (2004) Purification and analysis of a phospholipase A2-like lytic factor of *Trichomonas vaginalis*. *Infection and Immunity* **72**, 1284–1290.

Madico G, Quinn TC, Rompalo A, McKee KT and Gaydós CA (1998) Diagnosis of *Trichomonas vaginalis* infection by using vaginal swab samples. *Journal of Clinical Microbiology* **36**, 3205–3210.

Mallinson DJ, Lockwood BC, Coombs GH and North MJ (1994) Identification and molecular cloning of four cysteine proteinase genes from the pathogenic protozoon *Trichomonas vaginalis*. *Microbiology (Reading, England)* **140**, 2725–2735.

Mendoza-López MR, Becerril-García C, Fattel-Facenda LV, Ávila-González L, et al. (2000) CP30, A cysteine proteinase involved in *Trichomonas vaginalis* cytoadherence. *Infection and Immunity* **68**, 4907–4912.

Meza-Cervantez P, González-Robles A, Cárdenas-Guerra RE, Ortega-López J, Saavedra E, Pineda E and Arroyo R (2011) Pyruvate:ferredoxin oxidoreductase (PFO) is a surface-associated cell-binding protein in *Trichomonas vaginalis* and is involved in trichomonal adherence to host cells. *Microbiology (Reading, England)* **157**, 3469–3482.

Miranda-Ozuna JFT, Hernández-García MS, Brieba LG, Benítez-Cardoza CG, Ortega-López J, González-Robles A and Arroyo R (2016) The glycolytic enzyme triosephosphate isomerase of *Trichomonas vaginalis* is a surface-associated protein induced by glucose that functions as a laminin- and fibronectin-binding protein. *Infection and Immunity* **84**, 2878–2894.

Miranda-Ozuna JFT, Rivera-Rivas LA, Cárdenas-Guerra RE, Hernández-García MS, Rodríguez-Cruz S, González-Robles A, Chávez-Munguía B and Arroyo R (2019) Glucose-restriction increases *Trichomonas vaginalis* cellular damage towards HeLa cells and proteolytic activity of cysteine proteinases (CPs), such as TvCP2. *Parasitology* **146**, 1156–1166.

Neale KA and Alderete JF (1990) Analysis of the proteinases of representative *Trichomonas vaginalis* isolates. *Infection and Immunity* **58**, 157–162.

Ortíz-Estrada G, Calderón-Salinas V, Shibayama-Salas M, León-Sicairos N and De la Garza M (2015) Binding and endocytosis of bovine hololactoferrin by the parasite *Entamoeba histolytica*. *Biomedical Research International* **2015**, 375836.

Pastorek L, Sobol M and Hozák P (2016) Colocalization coefficients evaluating the distribution of molecular targets in microscopy methods based on pointed patterns. *Histochemical Cell Biology* **146**, 391–406.

Petrin D, Delgaty K, Bhatt R and Garber G (1998) Clinical and microbiological aspects of *Trichomonas vaginalis*. *Clinical Microbiology Reviews* **11**, 300–317.

Puente-Rivera J, Ramón-Luing LA, Figueroa-Angulo EE, Ortega-López J and Arroyo R (2014) Trichocystatin-2 (TC-2): an endogenous inhibitor of cysteine proteinases in *Trichomonas vaginalis* is associated with TvCP39. *International Journal of Biochemistry and Cell Biology* **54C**, 255–265.

Puente-Rivera J, Villalpando JL, Villalobos-Osnaya A, Vázquez-Carrillo LI, León-Avila G, Ponce-Regalado MD, López-Camarillo C, Elizalde-Contreras JM, Ruiz-May E, Arroyo R and Alvarez-Sánchez ME (2017) The 50 kDa metalloproteinase TvMP50 is a zinc-mediated *Trichomonas vaginalis* virulence factor. *Molecular Biochemical Parasitology* **217**, 32–41.

Ramón-Luing LA, Rendón-Gandarilla FJ, Puente-Rivera J, Ávila-González L and Arroyo R (2011) Identification and characterization of the immunogenic cytotoxic TvCP39 proteinase gene of *Trichomonas vaginalis*. *International Journal of Biochemistry and Cell Biology* **43**, 1500–1511.

Ramón-Luing LA, Rendón-Gandarilla FJ, Cárdenas-Guerra RE, Rodríguez-Cabrera N, Ortega-López J, et al. (2010) Immunoproteomics of the active degradome to identify biomarkers for *Trichomonas vaginalis*. *Proteomics* **10**, 435–444.

Rendón-Gandarilla FJ, Ramón-Luing LA, Ortega-López J, Rosa de Andrade I, Benchimol M and Arroyo R (2013) The TvLEGU-1, a legumain-like cysteine proteinase, plays a key role in *Trichomonas vaginalis* cytoadherence. *Biomed Research International* **2013**, 561979. doi: 10.1155/2013/561979.

Ryu JS, Choi HK, Min DY, Ha SE and Ahn MH (2001) Effect of iron on the virulence of *Trichomonas vaginalis*. *Journal of Parasitology* **87**, 457–460.

Sánchez-Rodríguez DB, Ortega-López J, Cárdenas-Guerra RE, Reséndiz-Cardiel G, Chávez-Munguía B, Lagunes-Guillén A and Arroyo R (2018) Characterization of a novel endogenous cysteine proteinase inhibitor trichocystatin-3 (TC-3), localized on the surface of *Trichomonas vaginalis*. *International Journal of Biochemistry and Cell Biology* **102**, 87–100.

Singh M, Sharma H and Singh N (2007) Hydrogen peroxide induces apoptosis in HeLa cells through mitochondrial pathway. *Mitochondrion* **7**, 367–373.

Solano-González E, Burrola-Barraza E, León-Sicairos C, Ávila-González L, Gutiérrez-Escolano L, Ortega-López J and Arroyo R (2007) The trichomonad cysteine proteinase TvCP4 transcript contains an iron-responsive element. *FEBS Letters* **581**, 2919–2928.

Sommer U, Costello CE, Hayes GR, Beach DH, Gilbert DO, *et al.* (2005) Identification of *Trichomonas vaginalis* cysteine proteases that induce apoptosis in human vaginal epithelial cells. *Journal of Biological Chemistry* **280**, 2853–2860.

Torres-Romero JC and Arroyo R (2009) Responsiveness of *Trichomonas vaginalis* to iron concentrations: evidence for a post-transcriptional iron regulation by an IRE/IRP-like system. *Infection Genetics and Evolution* **9**, 1065–1074.

Tsai CD, Liu HS and Tai JH (2002) Characterization of an iron-responsive promoter in the protozoan pathogen *Trichomonas vaginalis*. *Journal of Biological Chemistry* **277**, 5153–5162.

World Health Organization (2012) A baseline report on global sexually transmitted infection surveillance.